Use of Anodic TiO2 Nanotube Layers as Mesoporous Scaffolds for Fabricating CH3NH3PbI3 Perovskite-Based Solid-State Solar Cells

10 AUTHORS, INCLUDING:

Nhat Truong Nguyen
Friedrich-Alexander-University of Erlangen-…
11 PUBLICATIONS   30 CITATIONS

Mohamed Mokhtar
King Abdulaziz University
118 PUBLICATIONS   353 CITATIONS

Shaeel Al-thabaiti
King Abdulaziz University
205 PUBLICATIONS   514 CITATIONS

Patrik Schmuki
Friedrich-Alexander-University of Erlangen-…
581 PUBLICATIONS   19,565 CITATIONS

Use of Anodic TiO$_2$ Nanotube Layers as Mesoporous Scaffolds for Fabricating CH$_3$NH$_3$PbI$_3$ Perovskite-Based Solid-State Solar Cells

Raul Salazar,[a] Marco Altomare,[a] Kiyoung Lee,[a] Jyotsna Tripathy,[a] Robin Kirchgeorg,[a] Nhat Truong Nguyen,[a] Mohamed Mokhtar,[b] Abdelmohsen Alshehri,[b] Shaeel A. Al-Thabaiti,[b] and Patrik Schmuki*[a, b]

We optimize the deposition of CH$_3$NH$_3$PbI$_3$ perovskite into mesoporous electrodes consisting of anodic TiO$_2$ nanotube layers. By a simple spin-coating approach, complete filling of the tube scaffolds is obtained, which leads to interdigitated perovskite structures in conformal contact with the TiO$_2$ tube counterparts. Such assemblies can be used as solid-state solar cells in a hole-transporting-material-free configuration, that is, the tube scaffold serves as electron collector and blocking layer, while the perovskite acts as visible-light absorber and hole-transporting material. We show that the complete filling of the tube scaffold with the perovskite is essential to improve the solar cell efficiency.

1. Introduction

Significant improvements in the evolution of photovoltaic technology have been recently achieved by introducing perovskite-based materials in solar cell fabrication. In fact, the outstanding properties of these organo-metal halide light absorbers have, in a few years, led from low efficiency ($\eta = 3.7\%$) DSSC-version devices with a short operation lifetime to more robust solid-state solar cells that can reach power conversion efficiencies exceeding 16%[1–3] (cell efficiencies can in principle be pushed toward 20%).[4, 5]

Key advantages of using a perovskite sensitizer are its efficient charge transport properties and light absorption ability,[5] and well-developed solar cell geometry implies a planar thin-film configuration in which the TiO$_2$ electrode typically consists of a submicrometer nanoparticle layer.[6]

However, the use of one-dimensional (1D) TiO$_2$ nanostructures (e.g., nanorods, nanowires and nanotubes)[7–9] may be advantageous. With such electrodes it is possible for instance to deposit larger amounts of perovskite, with the aim of improving the light-absorption ability. Moreover, 1D TiO$_2$ nanostructures are also promising candidates as electron-collector scaffolds, owing to their directional charge transport properties.[9, 10] Besides, a 1D TiO$_2$ electrode can still assume the role of "blocking layer", that is, it minimizes the occurrence of electrical short-circuiting.[11, 12]

Over the past few years, self-ordered anodic TiO$_2$ nanotube (NT) layers have attracted wide interest, due to their facile production and a wide range of control over their geometry.[13] In this work we discuss the optimization of the perovskite deposition into anodic TiO$_2$ nanotube scaffolds and study the feasibility of realizing hole transport material (HTM)-free perovskite-based solar cells: the perovskite acts as visible-light absorber and hole-transporting material.[14] In general, perovskite solar cells that are electrolyte-based show a loss of efficiency over time that is ascribed to the chemical instability of the perovskite material.[1, 15] Therefore, as shown in Figure 1a, a solid-state configuration for the solar cells (i.e., electrolyte-free) was adopted. Clearly, the absence of liquid electrolyte and HTM makes mandatory the achievement of complete perovskite filling within the anodic tube scaffold, which is important for providing efficient hole transport (through the perovskite) and collection at the Au cathode (and also to prevent efficiency loss by short-circuiting).

2. Results and Discussion

Vertically aligned TiO$_2$ nanotube layers, as those shown in Figure 1 and Figure 2, with individual tube diameter of ca. 60–80 nm were grown by electrochemical anodization of Ti films (deposited on FTO slides) at 60 V, in an NH$_4$F-containing ethylene-glycol-based electrolyte (see the Experimental Section). Different lengths of the nanotubes were examined by tuning the thickness of the evaporated Ti films on FTO, that is, metal films with thicknesses of ca. 0.2, 0.4 and 1 μm were completely

[a] Dr. R. Salazar,$^+$ Dr. M. Altomare,$^+$ Dr. K. Lee, Dr. J. Tripathy, Dr. R. Kirchgeorg, N. T. Nguyen, Prof. Dr. P. Schmuki
Department of Materials Science and Engineering
WW4-LKO, University of Erlangen-Nuremberg
Martensstrasse 7, 91058 Erlangen (Germany)
Tel.: (+49)-9131-852-7575
Fax: (+49)-9131-852-7582
E-mail: schmuki@ww.uni-erlangen.de

[b] Prof. Dr. M. Mokhtar, Prof. Dr. A. Alshehri, Prof. Dr. S. A. Al-Thabaiti, Prof. Dr. P. Schmuki
Department of Chemistry
King Abdulaziz University
Jeddah (Saudi Arabia)

[$^+$] These authors contributed equally
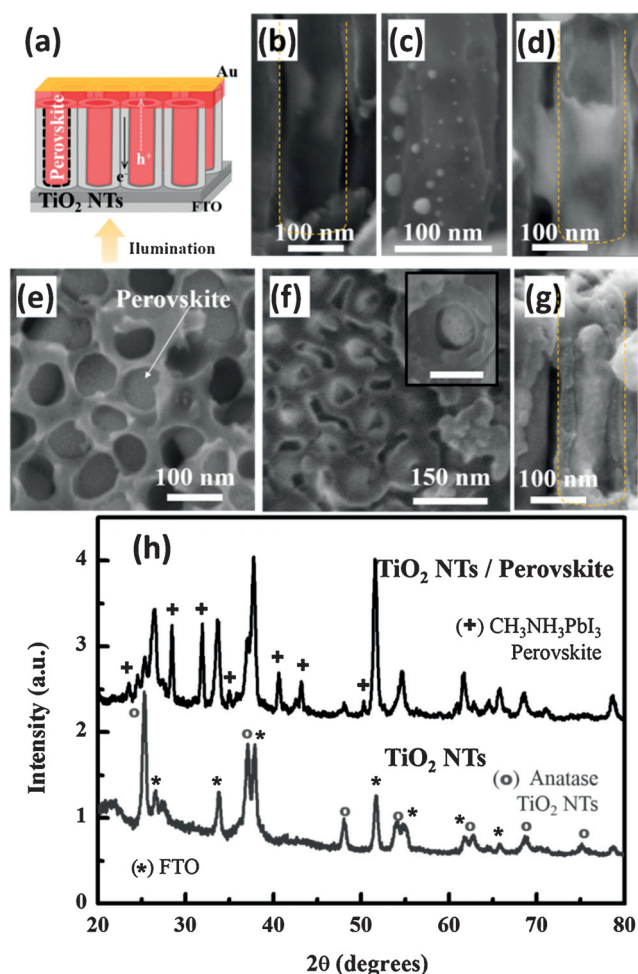
Figure 1. Schematic illustration of the solid-state HTM-free perovskite-based solar cell fabricated from a TiO$_2$ NT scaffold (a). Scanning electron microscopy (SEM) images of TiO$_2$ nanotubes after deposition of CH$_3$NH$_3$PbI$_3$ from: b),c) 10 wt% solution); d) 20 wt% solution; e)–g) 40 wt% solution e)–g). The inset in (f) shows a high-magnification SEM image of the bottom of a nanotube hosting the perovskite (the scale bar is 100 nm). h) X-ray diffraction patterns of a crystalline TiO$_2$ NT scaffold before and after deposition of the CH$_3$NH$_3$PbI$_3$ perovskite.

anodized. The complete anodization of Ti films precedes the exposure of the underlying conductive FTO layer to the electrolyte that would in turn lead to sudden increase of the current density—just prior to this, the anodization experiments were terminated. This resulted in the formation of 0.4, 1 and 2 μm-thick TiO$_2$ nanotube layers. The increase of layer thickness (with respect to the Ti film thickness) is due to the volume expansion typically observed when anodically growing TiO$_2$ nanotube layers.[13,16]

As anticipated above, in order to fabricate a functional solar cell geometry (such as in Figure 1a), we found that a most relevant key is to optimize the perovskite deposition approach,[17] towards complete filling of the TiO$_2$ tube scaffolds. Therefore, spin-coating deposition was investigated using perovskite solutions of different concentrations. Figures 1b–g show 0.4 μm-thick TiO$_2$ nanotube layers that were coated with 10, 20 and 40 wt% CH$_3$NH$_3$PbI$_3$ perovskite solutions.

When a 10 wt% solution was used, the walls of the tubes could be decorated with isolated perovskite nanocrystals of rather broad size distribution, namely, in the 2–17 nm range (Figure 1b and Figure 1c). This morphology is typically observed when a classic mesoporous particle template is used.[15]

When depositing 20 wt% solutions, a nearly complete filling was obtained (Figure 1d). However, some voids were still left in the perovskite structure, most likely due to solvent evaporation upon annealing (as outlined in the Experimental Section, the annealing step is required for crystallizing the perovskite). In other words, perovskite concentrations of up to 20 wt% did not lead to a continuous perovskite filling, which is expected to be essential for the cell functionality (indeed, incomplete filling detrimentally affects the solar cell efficiency).

As shown in Figures 1e–g, complete filling of the tubes was obtained by using 40 wt% solutions. In this case the perovskite material could be confined in the TiO$_2$ scaffolds and the 0.4 μm-thick tubes were fully filled, from the very bottom to the top, leading to a perovskite morphology that resembles a replica of the tube scaffold. Noteworthy, we could finely cast the perovskite shape by using a single-step deposition method (and a tube layer template), which clearly simplifies the solar cell processing compared to a previously reported multi-step solution-based approach.[2]

The effective deposition and crystallization of the perovskite was confirmed by means of X-ray diffractometry (see the XRD patterns of crystalline TiO$_2$ tube scaffolds before and after perovskite deposition in Figure 1h).[15]

In order to complete the solar cell fabrication, we sputter-coated Au electrodes (100 nm-thick) onto the assemblies (Figure 1a). J–V curves of the device were then measured under AM 1.5 simulated solar light irradiation, as shown in Figure 2a. Overall, solar cells fabricated by depositing the perovskite into the TiO$_2$ tube scaffolds from 10 wt% solutions showed no photoresponse. This can be explained by considering that the perovskite deposition from 10 wt% solutions leads only to isolated nanosized crystals that do not provide a continuous medium for hole transport. Moreover, the ohmic behavior observed in the J–V curves is likely the result of a direct contact between the TiO$_2$ scaffold and the Au electrode (i.e., in the presence of a poor perovskite filling, not only does the sputtered Au directly coat the TiO$_2$ tubes but it may even reach locations deep within the mesoporous scaffold). Thus, for an ideal perovskite filling and, at the same time, not to compromise the solar cell functionality, we found it important to prevent electrical shunts ascribed to direct contact between the electron collector and the Au electrode.

For this, not only did we optimize the perovskite deposition to obtain complete filling of the tube layers (this aspect is discussed later) but we also extended the deposition of the perovskite to form a capping layer, of different thicknesses, over the tube scaffold (Figures 2b,c). In principle, such a perovskite over-layer should be sufficiently thick to optimize the light absorption and prevent electrical shunts, but should also be thin enough to grant effective hole transport towards the Au electrode.[2,18]
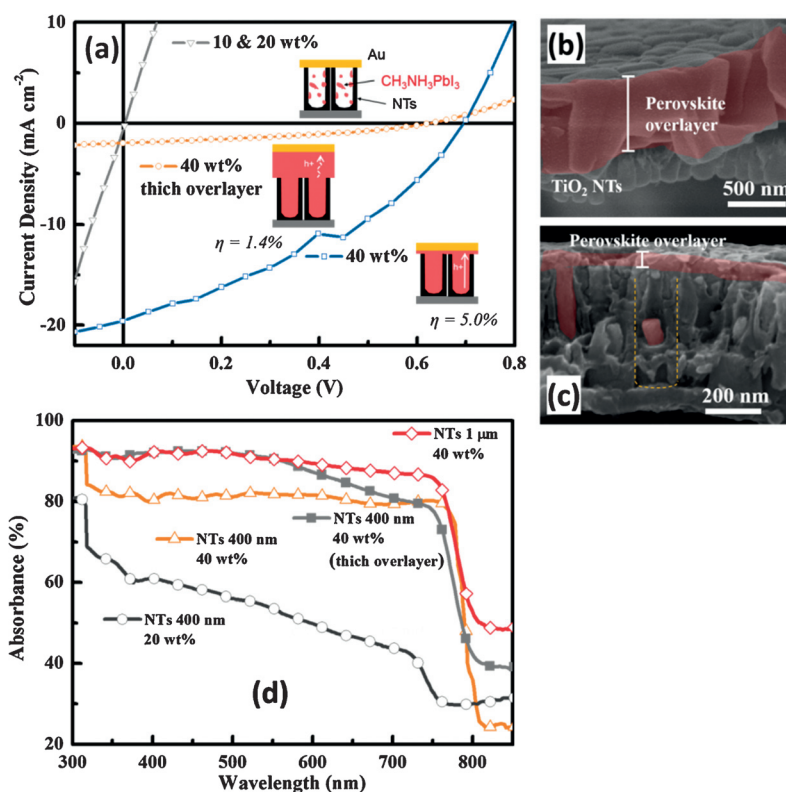
Figure 2. a) Current density–voltage curves of HTM-free perovskite-based solar cells fabricated from 0.4 μm-thick TiO$_2$ nanotube scaffolds filled with perovskite material by a spin-coating approach. Cross-sectional SEM images of b) thick and c) thin perovskite layers deposited over TiO$_2$ NT scaffolds using a 40 wt% solution, by a spin-coating approach carried out at 2000 and 3000 rpm, respectively. d) UV/Vis spectra of TiO$_2$ NT scaffolds of different thickness, sensitized with different amounts of CH$_3$NH$_3$PbI$_3$ perovskite.
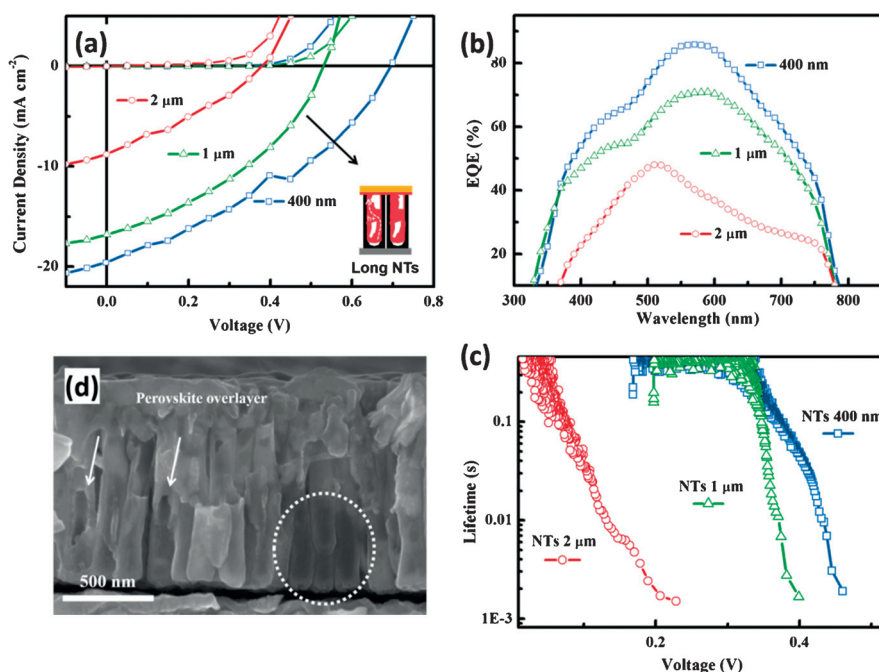
Figure 3. a) Current density–voltage curves and b) EQE spectra of HTM-free perovskite-based solar cell fabricated from TiO$_2$ NT layers of different thickness (the concentration of the spin-coated perovskite solution is 40 wt%). c) Electron lifetime of HTM-free CH$_3$NH$_3$PbI$_3$ perovskite-based solar cells fabricated from tube layers of different thicknesses. d) Cross-sectional SEM image of a 1 μm thick TiO$_2$ tube layer after deposition of CH$_3$NH$_3$PbI$_3$ from 40 wt% solution (arrows and dotted area indicate empty space within the NTs).

We found that a >500 nm-thick perovskite over-layer (Figure 2b) resulted in relatively low short-circuit current density (J_{sc}) and efficiency (η) (Figure 2a), this although such geometry shows excellent light absorbance (Figure 2d). In fact, this thick over-layer most likely limits the hole transport and consequently leads to relatively low J_{sc}. Instead, thinner perovskite over-layers (<100 nm-thick, see Figure 2c) yielded a much higher J_{sc} of ca. 19 mA cm^{-2}, resulting in our highest cell efficiency of 5.0% (Figure 2a).

Slightly higher efficiencies (ca. 6.5%) were recently reported for solar cells fabricated by depositing the perovskite absorber into anodic TiO$_2$ nanotube membranes:[9] the scope of that work was not that of optimizing the light absorber deposition, and therefore only a limited perovskite filling was obtained, which resembles the structures we prepared in the present study using a 10 wt% perovskite solution (Figure 1c). Moreover, these results were achieved with electrolyte-based solar cells that also showed a dramatic loss of efficiency over time, ascribed to the perovskite decomposition.[1, 15]

The effect of the TiO$_2$ scaffold structure was also investigated and solar cells were fabricated from thicker tube layers. Although these layers showed superior absorbance features (Figure 2d), they provided significantly lower efficiencies compared to shorter (0.4 μm-thick) tubes (Figure 3a, Table 1)Table in Figure moved to a separate Table (Table 1), house style. Data in Figure 3b confirm that clearly higher external quantum efficiency (EQE) was measured for thin tube scaffolds. Note that EQE results for devices based on 0.4 μm-thick tubes closely match the corresponding UV/Vis absorption spectrum, this in terms of EQE offset (see Figures 2d

Table 1. Photovoltaic parameters of HTM-free perovskite-based solar cell fabricated from TiO_2 NT layers of different thickness (the concentration of the spin-coated perovskite solution is 40 wt %).

	V_{oc} [V]	J_{sc} [mA cm^{-2}]	FF [%]	PCE [%]
0.4 μm	0.67	19.6	37	5.0
1.0 μm	0.55	16.7	37	3.4
2.0 μm	0.37	8.8	28	1.0

and 3b for comparison). Solar cells fabricated from 1 and 2 μm-thick tubes showed instead lower cell efficiencies and EQE and, in particular, the latter exhibited unexpectedly lower EQE values in the 600–800 nm range. In other words, thicker tube layers led to promising improvement of light absorption ability but exhibited at the same time a dramatic worsening of the charge collection efficiency—this can be argued also from the V_{oc} and FF data, which significantly decreased with increasing the thickness of the tube scaffold (Figure 3a), confirming that the rate of charge extraction is limited when using thicker tube electrodes.[3]

Therefore, to further investigate the performance of our solar cells, photo-induced open-circuit voltage decay measurements were carried out.[19] The results (Figure 3c) show that the carrier lifetime tends to decrease as the thickness of the tube scaffold increases. In principle, no significant difference in tube electron transport property is expected to be observed when tube length varies only slightly (i.e., from 0.4 to 2 μm).[13, 16, 20] These non-ideal results can be ascribed to the non-optimized perovskite deposition into the thicker nanotube scaffolds, meaning that the perovskite structure presents voids and discontinuities (as shown in Figure 3d),[9] so that the hole transport and collection is hindered.

Noteworthy, it was recently shown that 2 μm-thick perovskite-sensitized TiO_2 nanotube layers are able to absorb nearly 90 % of the incident UV/Vis light (and to efficiently convert it into photocurrent).[9] Therefore, the optimization of the perovskite deposition technique in order to conformally fill even thicker tube layers is undoubtedly the next challenge to tackle, in view of pushing the solar cell efficiencies of all-solid-state solar cells to higher values. Even more, on the basis of recent findings, further improvements may also be pursued by enhancing the electronic properties of the anodic TiO_2 nanotube scaffolds (e.g., by using single-walled tubes,[21, 22] and/or by an optimized thermal treatment of the tube scaffolds).[23]

3. Conclusions

We fabricated perovskite-based solar cells by using anodic TiO_2 nanotube layers as blocking layer and electron collector scaffolds. By optimizing a spin-coating deposition, we could obtain interdigitated and continuous perovskite structures in intimate contact with the nanotube counterparts, and construct solid-state solar cells without the use of hole-transporting material. For solar cells fabricated from 0.4 μm-thick tube scaffolds we reached a short-circuit current density and an efficiency of 19 mA cm^{-2} and 5.0 %, respectively. Such relatively high current density is more likely ascribed to the large amount of perov-

skite material deposited in intimate contact with the nanotube electrode. We envisage a further optimization of the perovskite deposition, along with the use of thicker TiO_2 nanotube scaffolds, as the next step to explore in view of fabricating solid-state solar cells with enhanced power conversion efficiencies.

Experimental Section

Transparent TiO_2 nanotube layers were grown by electrochemical anodization of Ti films (thickness of 0.2, 0.5 and 1 μm) that were deposited by electron beam evaporation on FTO glass (TCO22–15, Solaronix). The deposition rate was 0.6 nm min^{-1} at $5 \times 10^{-7} - 2 \times 10^{-6}$ mbar (Fraunhofer Institute for Integrated Systems, Erlangen, Germany). Prior to the Ti evaporation, the FTO substrates were cleaned (in acetone, ethanol and deionized water, for 15 min each) and coated with a compact layer of TiO_2 by spin-coating, using titanium diisopropoxide bis(acetylacetonate) (Aldrich, 75 wt % in isopropanol) dissolved in 1-butanol (Aldrich, 99.8 %). The TiO_2 compact film enhances the adhesion of the nanotube scaffold to the FTO glass, and also serves as blocking layer. The anodization experiments to grow TiO_2 NT layers were carried out in a two-electrode electrochemical cell with a Pt foil as cathode and the Ti/FTO layers as anode. The anodization voltage was 60 V and the electrolyte was composed of 0.15 mM NH_4F (Sigma–Aldrich), 3 vol % deionized (DI) water and ethylene glycol (99.8 % purity, <1 % H_2O; Fluka). After anodization, the TiO_2 NT layers were rinsed overnight in ethanol to desorb the electrolyte. Afterwards, the samples were dried in a N_2 stream and annealed in air at 450 °C for 1 h.

The synthesis of the $CH_3NH_3PbI_3$ light absorber is reported elsewhere.[17] Briefly, CH_3NH_3I was synthesized by mixing 30 mL of hydriodic acid (37 %, Sigma Aldrich) and 27.8 mL of methylamine (40 % in methanol, TCI) in an ice bath for 2 h. Subsequently, the solvent was evaporated by placing the solution in an evaporator at 60 °C. The CH_3NH_3I product was washed with diethyl ether and dried in vacuum. For the synthesis of the $CH_3NH_3PbI_3$, solution of 10, 20, 40 and 60 wt % of CH_3NH_3I were mixed to PbI_2 (99 % Sigma Aldrich) in N,N-dimethylformamine (DMF). To prepare a 10 wt % solution, 0.5 g of CH_3NH_3I and 1.4 g of PbI_2 were mixed in 10 mL of solvent.

For the solar cell fabrication, $CH_3NH_3PbI_3$ solutions were spin-coated onto the TiO_2 NT scaffolds (2000 rpm, 30 s). The samples were then annealed at 100 °C for 20 min. The fabrication of the solar cells was completed by sputtering a Au layer (100 nm) on the top of the device (i.e., onto the perovskite overlayer) as counter electrode (see a sketch of the solar cell in Figure 1a).

The nanostructures were characterized using a field-emission scanning electron microscope (Fe-SEM, S4800, Hitachi) and an X-ray diffractometer (XRD, X'pert Philip MPD with a Panalytical X'celerator detector and graphite monochromized CuKα radiation, $\lambda =$ 1.54056 Å). UV/Vis absorption spectra were recorded using a Perki-nElmer UV/Vis spectrometer with integrating sphere. Photocurrent density–voltage ($J–V$) measurements were carried out under AM 1.5 illumination provided by a solar simulator (300 W Xe with optical filter, Solarlight) applying an external bias to the cell and measuring the generated photocurrent with a Keithley model 2420 digital source meter. Prior to measurement, the solar simulator was calibrated using a reference solar cell (OPRC22Si-CAL; Optopolymer). The irradiated area of the solar cells was 0.16 cm² (masking conditions). The external quantum efficiency (EQE) characterization was performed using an EQE Measurement System (Enlitech) equipped with a Xe lamp. Photo-induced open-circuit voltage

decay measurements were carried out using a Autolab PGSTAT 30 Potentiostat/Galvanostat (Ecochemie, The Netherlands) under AM 1.5 illumination provided by a solar simulator (300 W Xe with optical filter, Solarlight).

Acknowledgements

[1] A. Kojima, K. Teshima, Y. Shirai, T. Miyasaka, *J. Am. Chem. Soc.* **2009**, *131*, 6050 – 6051.

[2] N. J. Jeon, J. H. Noh, Y. C. Kim, W. S. Yang, S. Ryu, S. Il Seok, *Nat. Mater.* **2014**, *13*, 897 – 903.

[3] J.-H. Im, I.-H. Jang, N. Pellet, M. Grätzel, N.-G. Park, *Nat. Nanotechnol.* **2014**, *9*, 927 – 932.

[4] N. Park, *J. Phys. Chem. Lett.* **2013**, *4*, 2423 – 2429.

[5] H. Snaith, *J. Phys. Chem. Lett.* **2013**, *4*, 3623 – 3630.

[6] M. Liu, M. B. Johnston, H. J. Snaith, *Nature* **2013**, *501*, 395 – 398.

[7] J. Qiu, Y. Qiu, K. Yan, M. Zhong, C. Mu, H. Yan, S. Yang, *Nanoscale* **2013**, *5*, 3245 – 3248.

[8] H. Kim, J. Lee, N. Yantara, P. Boix, *Nano Lett.* **2013**, *13*, 2412 – 2417.

[9] X. Gao, J. Li, J. Baker, Y. Hou, D. Guan, J. Chen, C. Yuan, *Chem. Commun.* **2014**, *50*, 6368 – 6371.

[10] M. Law, L. E. Greene, J. C. Johnson, R. Saykally, P. Yang, *Nat. Mater.* **2005**, *4*, 455 – 459.

[11] J.-W. Lee, T.-Y. Lee, P. J. Yoo, M. Grätzel, S. Mhaisalkar, N.-G. Park, *J. Mater. Chem. A* **2014**, *2*, 9251.

[12] B. Peng, G. Jungmann, C. Jäger, D. Haarer, H.-W. Schmidt, M. Thelakkat, *Coord. Chem. Rev.* **2004**, *248*, 1479 – 1489.

[13] K. Lee, A. Mazare, P. Schmuki, *Chem. Rev.* **2014**, *114*, 9385 – 9454.

[14] L. Etgar, P. Gao, Z. Xue, Q. Peng, A. K. Chandiran, B. Liu, M. K. Nazeeruddin, M. Grätzel, *J. Am. Chem. Soc.* **2012**, *134*, 17396 – 17399.

[15] J.-H. Im, C.-R. Lee, J.-W. Lee, S.-W. Park, N.-G. Park, *Nanoscale* **2011**, *3*, 4088 – 4093.

[16] P. Roy, S. Berger, P. Schmuki, *Angew. Chem. Int. Ed.* **2011**, *50*, 2904 – 2939; *Angew. Chem.* **2011**, *123*, 2956 – 2995.

[17] H.-S. Kim, C.-R. Lee, J.-H. Im, K.-B. Lee, T. Moehl, A. Marchioro, S.-J. Moon, R. Humphry-Baker, J.-H. Yum, J. E. Moser, M. Grätzel, N.-G. Park, *Sci. Rep.* **2012**, *2*, 591.

[18] W. A. Laban, L. Etgar, *Energy Environ. Sci.* **2013**, *6*, 3249.

[19] J. Mahan, T. Ekstedt, *IEEE Trans. Electron Devices* **1979**, *26*, 733 – 739.

[20] K. Zhu, N. Neale, A. Miedaner, A. Frank, *Nano Lett.* **2007**, *7*, 69 – 74.

[21] N. Liu, H. Mirabolghasemi, K. Lee, S. P. Albu, A. Tighineanu, M. Altomare, P. Schmuki, *Faraday Discuss.* **2013**, *164*, 107 – 116.

[22] S. So, I. Hwang, P. Schmuki, *Energy Environ. Sci.* **2015**, DOI: 10.1039/c4ee03729d.

[23] F. Mohammadpour, M. Moradi, K. Lee, G. Cha, S. So, A. Kahnt, D. M. Guldi, M. Altomare, P. Schmuki, *Chem. Commun.* **2015**, *51*, 1631 – 1634.